Atmospheric
Chemistry
and Physics
Discussions

Impact of Gobi desert dust on aerosol chemistry of Xi'an, inland China during spring 2009: differences in composition and size distribution between the urban ground surface and the mountain atmosphere

G. H. Wang[1], B. H. Zhou[2,3], C. L. Cheng[1], J. J. Cao[1], J. J. Meng[1], J. J. Li[1], J. Tao[4], R. J. Zhang[5], and P. Q. Fu[6]

[1]State Key Laboratory of Loess and Quaternary Geology, Institute of Earth Environment, Chinese Academy of Sciences, Xi'an 710075, China
[2]School of Environmental and Municipal Engineering, Xi'an University of Architecture and Technology, Xi'an 710055, China
[3]Department of Geographical Science and Environmental Engineering, Baoji University of Arts and Sciences, Baoji 721013, China
[4]South China Institute of Environmental Sciences, China Ministry of Environmental Protection, Guangzhou 510655, China

Title Page

Abstract | Introduction

Conclusions | References

Tables | Figures

|◄ | ►|

◄ | ►

Back | Close

Full Screen / Esc

Printer-friendly Version

Interactive Discussion

[5]Key Laboratory of Regional Climate-Environment for Temperate East Asia, Institute of Atmospheric Physics, Chinese Academy of Sciences, Beijing 100029, China
[6]Institute of Atmospheric Physics, Chinese Academy of Sciences, Beijing 100029, China

Correspondence to: G. H. Wang (wanggh@ieecas.cn or gehuiwang@yahoo.com.cn)

Impact of Gobi desert dust on aerosol chemistry of Xi'an

G. H. Wang et al.

Title Page

Abstract	Introduction
Conclusions	References
Tables	Figures

⏮ ⏭

◀ ▶

Back Close

Full Screen / Esc

Printer-friendly Version

Interactive Discussion

Abstract

Composition and size distribution of atmospheric aerosols from Xi'an city (~ 400 m, altitude) in inland China during the spring of 2009 including a massive dust event on 24 April were measured and compared with a parallel measurement at the summit (2060 m, altitude) of Mt. Hua, an alpine site nearby Xi'an. EC, OC and major ions in the city were 2–22 times higher than those on the mountaintop during the whole sampling period. Sulfate was the highest species in the nonevent time in Xi'an and Mt. Hua, followed by nitrate, OC and NH_4^+. In contrast, OC was the most abundant in the event at both sites, followed by sulfate, nitrate and Ca^{2+}. Compared to those on the urban ground surface aerosols in the elevated troposphere over Mt. Hua contain more sulfate and less nitrate, because HNO_3 is formed faster than H_2SO_4 and thus long-range transport of HNO_3 is less significant than that of H_2SO_4. An increased water-soluble organic nitrogen (WSON) was observed for the dust samples from Xi'an, indicating a significant deposition of anthropogenic WSON onto dust and/or an input of biogenic WSON from Gobi desert.

As far as we know, it is for the first time to perform a simultaneous observation of aerosol chemistry between the ground surface and the free troposphere in inland East Asia. Our results showed that fine particles are more acidic on the mountaintop than on the urban ground surface in the nonevent, mainly due to continuous oxidation of SO_2 to produce H_2SO_4 during the transport from lowland areas to the alpine atmosphere. However, we found the urban fine particles became more acidic in the event than in the nonevent, in contrast to the mountain atmosphere, where fine particles were less acidic when dust was present. The opposite changes in acidity of fine particles at both sites during the event are mostly caused by enhanced heterogeneous formation of nitrate onto dust in the urban air and decreased formation of nitrate in the mountain troposphere. In comparison to those during the nonevent Cl^- and NO_3^- in the urban air during the event significantly shifted toward coarse particles. Such redistributions were further pronounced on the mountaintop when dust was present, resulting in both

Title Page

Abstract	Introduction
Conclusions	References
Tables	Figures

Back | Close

Full Screen / Esc

Printer-friendly Version

Interactive Discussion

ions almost entirely staying in coarse particles. On the contrary, no significant spatial difference in size distribution of SO_4^{2-} was found between the urban ground surface and the mountain atmosphere, dominating in the fine mode ($< 2.1\,\mu m$) during the nonevent and comparably distributing in the fine ($< 2.1\,\mu m$) and coarse ($> 2.1\,\mu m$) modes during the event.

1 Introduction

Dust is one of the major particulate matters in the atmosphere. Global annual mean burden of aerosol dust is about 20 Tg (δ 40 %) (Mcnaughton et al., 2009). These dusts can influence the solar radiation by directly absorbing/reflecting sunlight and indirectly acting as cloud condensation nuclei (CCN) or ice nuclei (IN) (Jacobson, 2001; Manktelow et al., 2010; Mcnaughton et al., 2009; Seinfeld et al., 2004). Furthermore, dusts are of adverse health effects since they can deposit into human respiratory tract and become more toxic after mixing with pollutants by absorption and reaction (Huebert et al., 2003). Gobi deserts located in South Mongolia and North China are one of the major source regions of East Asian dust (Arimoto et al., 2006; Sullivian et al., 2007). In each spring and early summer surface dust in Gobi desert region is brought about by front cold systems and the Mongolian cyclonic depression and transported into the downwind areas including North America (Leaitch et al., 2009; Seinfeld et al., 2004; Vancuren and Cahill, 2002). During the transport mineral dust can internally mix with secondary compounds such as ammonium sulfate, ammonium nitrate, carboxylic acids, nitrogen-containing organics and seal salt by coagulation, cloud-processing and heterogeneous reactions (Geng et al., 2009; Seinfeld et al., 2004; Sullivan et al., 2009; Tobo et al., 2010; Wang et al., 2012a, b; Zamora et al., 2011; Zhang et al., 2003). These processes modify the physicochemical properties of the airborne aerosols containing dust, exerting a significant impact on the downwind atmospheric environment (Dillner et al., 2006).

Field measurements of the Gobi dust have been performed at many sites from the source region in Northern/Northwestern China to North America. However, simultaneous observation for dust-laden aerosols between the boundary layer and the free troposphere has been conducted only in the Asian continental outflow region such as the ACE-Asia 2001 in Northwest Pacific (Huebert et al., 2003; Seinfeld et al., 2004; Simoneit et al., 2004a, b) and the INTEX-2006 in Northeast America (Dunlea et al., 2009; Peltier et al., 2008; Van Donkelaar et al., 2008), but there is no such a simultaneous measurement conducted in inland China. Located in Central China, Guanzhong Basin is one of the most polluted regions in the world, where annual average level of fine particles was more than $80\,\mu g\,m^{-3}$ in 2001–2006 (Van Donkelaar et al., 2010; Wang et al., 2006a, b, 2010). In the spring of 2009, an intensive observation of atmospheric aerosols was performed simultaneously in Xi'an, Mt. Hua and Mt. Tai, which are situated in Guanzhong Basin, inland China and North China Plain, East Coastal China, respectively, to identify the similarity and difference in chemical composition and size distribution of aerosols between the ground surface and the free troposphere (Wang et al., 2011c, 2012a, b). During the sampling period a massive dust storm originating from Gobi desert simultaneously occurred at the three sites. In our previous papers EC, OC, inorganic ions and organic aerosols in the two alpine atmospheres have been reported (Wang et al., 2011c, 2012b). Both Xi'an city and Mt. Hua are located within the same region, i.e. Guanzhong Basin, with a distance ~ 80 km. To recognize the difference in aerosol chemistry between the boundary layer and the free troposphere over Guanzhong Basin, here we first characterized composition and size distribution of airborne particles of Xi'an in the springtime of 2009, and then compared these urban results with those in the atmosphere over Mt. Hua. Our results demonstrated that dust storm has different effects on the chemical properties of aerosols between the ground surface (~ 400 m, a.s.l.) and the mountaintop troposphere (2060 m, a.s.l.) in inland China, resulting in acidity of fine particles increasing on the urban ground surface and decreasing in the mountaintop atmosphere when dust was present.

2 Experimental section

2.1 Collection of PM_{10} and size-segregated particles

Xi'an city is situated in Guanzhong Basin, a semi-arid region in Central China (Fig. 1). PM_{10} and 9-stage size-segregated samples were simultaneously collected on the rooftop (10 m above the ground) of a three-story building at Institute of Earth Environment in the urban area of Xi'an. The PM_{10} sample was collected on a day/night basis at an airflow rate of $100\,l\,min^{-1}$, while the size-segregated samples were collected for 4 days in each set at an airflow rate of $28\,l\,min^{-1}$ with 9 size bins as < 0.4, 0.4–0.7, 0.7–1.1, 1.1–2.1, 2.1–3.3, 3.3–4.7, 4.7–5.8, 5.8–9.0 and $> 9.0\,\mu m$, respectively. The sampling lasted for one month from 25 March to 25 April 2009. All the samples were collected onto pre-combusted (450 °C for 8 h) quartz fiber filters. The airflow rates of the two samplers were calibrated before and after the sampling to ensure the instruments working at the specified flow rates. After sampling, the filter was sealed in an aluminum foil bag and stored at −20 °C before analysis. The particle mass on the filter was gravimetrically measured using a microelectronic balance (Mettler M3, Swiss) with a sensitivity limit of 10 μg after a 24-h equilibration inside a chamber (RH = 50 ± 10 %, $T = 23$–25 °C).

During the sampling period, a moderate dust storm (Named as DS I, hereinafter) originating from Gobi desert reached Xi'an on 20 April, four days later a massive dust storm (Named as DS II, hereinafter), which also originated from Gobi desert, arrived in Xi'an (on 24 April). Both episodes also simultaneously occurred at Mt. Hua, 80 km east to the city (See Fig. 1). During the second event, the PM_{10} sampling duration was changed into 3–6 h depending on the particle loading, while the size-segregated sampling duration was changed into one day.

2.2 Sample analysis

2.2.1 Inorganic ions, water-soluble organic (WSOC) and inorganic carbon (WSIC), and water-soluble organic nitrogen (WSON)

One fourth of the filter was cut into pieces and extracted for three times with Milli-Q pure water under sonication. One part of the combined water-extracts was determined for inorganic ions using Dionex-6000 ion chromatography after a measurement of pH value using a pH meter (HANNA HI8424 pH meter, US) at an ambient temperature of 25 °C. Another part of the water-extracts was determined for water-soluble organic carbon (WSOC), water-soluble inorganic carbon (WSIC) and water-soluble total nitrogen (WSTN) using Shimadzu 5000 TOC/N Analyzer. The detailed analysis methods for inorganic ions, WSOC and WSTN can be found elsewhere (Wang et al., 2010). NO_3^- and NH_4^+ are the major water-soluble inorganic nitrogen (WSIN) species in atmospheric particles, thus the difference between WSTN and WSIN is defined as water-soluble organic nitrogen (WSON).

2.2.2 Organic carbon (OC) and elemental carbon (EC)

OC and EC in the PM_{10} samples were measured by a DRI Model 2001 Carbon Carbon Analyzer using the Interagency Monitoring of Protected Visual Environments (IMPROVE) thermal/optical reflectance (TOR) protocol (Chow et al., 2004, 2007). Briefly, a size of 0.53 cm^2 filter was put in a quartz boat inside the analyzer and progressively heated to temperatures of 120°, 250°, 450°, and 550° in a non-oxidizing helium (He) atmosphere, and 550°, 700°, and 800° in an oxidizing atmosphere containing 2 % oxygen in helium.

An intercomparison was made for the PM_{10} and the size-resolved samplers. As shown in Fig. 2, a linear correlation was observed for particle mass (PM) and major species measured by the two samplers with a slope close to unity, indicating a good agreement between the two data sets. A parallel observation was performed at the

Impact of Gobi desert dust on aerosol chemistry of Xi'an

G. H. Wang et al.

Title Page

Abstract	Introduction
Conclusions	References
Tables	Figures

◀◀   ▶▶

◀   ▶

Back   Close

Full Screen / Esc

Printer-friendly Version

Interactive Discussion

summit (2060 m a.s.l.) of Mt. Hua using the same sampling instruments (Wang et al., 2011c, 2012b), and the related data are cited here to investigate the difference in composition and size distribution between the urban ground surface and the elevated mountaintop troposphere.

3 Results and discussion

3.1 Chemical composition of PM_{10}

Temporal variation of PM_{10} is presented in Fig. 3, and the chemical component concentrations are summarized in Table 1. PM_{10} ranged from 58 to 420 $\mu g\,m^{-3}$ in the nonevent time with EC and OC as high as 29 and 67 $\mu g\,m^{-3}$, respectively, suggesting a high loading of pollutants in the city. As seen in Table 1, there is no significant difference in the concentrations between day and night during the non-dust storm period, which is mostly due to the stagnant meteorological conditions within the basin-like region. The daytime and nighttime OC/EC ratios were 2.5 ± 0.6 and 2.3 ± 0.7 during the nonevent period, respectively. Relative abundance of water-soluble organic nitrogen (WSON) to water-soluble total nitrogen (WSTN) were 0.3 ± 0.2 and 0.4 ± 0.2 in the day- and night-samples during the non-dust storm period (Table 1), suggesting that inorganic nitrogen compounds, i.e. nitrate and ammonium, are the major nitrogen-containing species in the atmosphere during the nonevent period. However, WSON/WSTN ratios increased to 0.7 and 0.7 ± 0.3 in the DS I and DS II episodes, respectively, indicating that organic nitrogen species during the events were more abundant than ammonium and nitrate. The absolute concentration of WSON was 8.1 and 19 ± 12 $\mu g\,m^{-3}$ during the two events, respectively, which is 2–5 times higher than that in the nonevent especially in the DS II event. Such an enhancement of WSON was also observed in Miami and Barbados (Zamora et al., 2011) and Eastern Mediterranean (Violaki and Mihalopoulos, 2010) when Africa dust presented. Mass closure analysis further showed that the sum of total inorganic ions, EC and organic matter (OM) accounted for over 70 % of

PM_{10} mass with the remaining being insoluble mineral dust (Fig. 4a, b), in contrast to that in the dust periods, which was only 23 % and 24 % in the DS I and DS II events, respectively (Fig. 4c, d).

Figure 5 compares differences in the concentrations of major aerosols in Xi'an with those in Mt. Hua during the same periods. In the nonevent time PM_{10} in Xi'an was 3.6 times that in Mt. Hua (Fig. 5a), and the most abundant species in the PM_{10} samples at both sites was SO_4^{2-}, followed by NO_3^-, OC and NH_4^+. EC was higher than Ca^{2+} in Xi'an but lower than Ca^{2+} in Mt. Hua. On the contrary, in the DS II time the most abundant species in the PM_{10} samples at both sites was OC, followed by SO_4^{2-}, Ca^{2+} and NO_3^- (Fig. 5b). Our previous study found that organic matters in the dust samples from Mt. Hua are mainly originated from Gobi plants (Wang et al., 2012b) and the increased alkaline ions like Ca^{2+} and Mg^{2+} are derived from heterogeneous reactions of acidic gases such as N_2O_5 and nitric and sulfuric acids with dust (Karagulian et al., 2006; Mogili et al., 2006). The spatial difference between Xi'an and Mt. Hua in the DS II event became less significant for all species except for F^- (see the inserted numbers).

NO_3^-/SO_4^{2-} molar ratio was 0.20–2.2 (average, 1.22 ± 0.48) in Xi'an and 0.19–1.4 (average, 0.60 ± 0.36) in Mt. Hua during the non-dust storm period. In the DS II period the ratio decreased to 0.97 ± 0.26 (range, 0.67–1.2) in Xi'an but was almost constant in Mt. Tai (0.68 ± 0.32, 0.43–1.0) compared to those in the nonevent. The major formation pathways of NO_3^- and SO_4^{2-} in the atmosphere are the photo-oxidation of NO_2 and SO_2 with OH radical (Formenti et al., 2010; Jockel et al., 2003; Seinfeld and Pandis, 1998), but the NO_3^- formation is about 10 times faster than that of SO_4^{2-} (Rodhe et al., 1981; Vrekoussis et al., 2004, 2007). Thus, higher level of NO_x in Xi'an tends to reduce the levels of OH and H_2O_2 in the urban air and delay the transformation of SO_2 to H_2SO_4, resulting in the relative abundance of nitrate being higher in the urban area and lower on the mountaintop. Such different reaction rates also suggest that nitrate formation is only significant close to the source area but sulfate formation is continuous during the transport. Moreover, sulfate is non-volatile and the strongest acid, once formed in the dust it may prevent other weaker acids like HNO_3 and HCl accumulate onto the

dust (Sullivian et al., 2007). Therefore, compared to that in the nonevent the smaller NO_3^-/SO_4^{2-} ratio in Xi'an during the DS II time reveals a relatively increased formation of sulfate during the long-range transport of dust storm.

As shown in Fig. 6a, particles in the mountain troposphere during the nonevent con-
tained more sulfate compared to those in the urban air, but relative abundance of am-
monium in the alpine PM_{10} samples was similar to that in the urban samples and nitrate
was less than that in the urban samples, probably indicating a displacement of am-
monium nitrate by ammonium bisulfate/sulfate during the transport of pollutants from
lowland region to the elevated troposphere and an evaporation of nitric acid from solid
phase to gas phase. During the DS II period the most significant differences in relative
abundance between the ground surface and the mountain troposphere were found for
F^- and EC (Fig. 6b), both were 9 times more abundant in the urban area than in the
alpine region (See Fig. 5b), suggesting that F^- and EC in Xi'an are largely originated
from the local sources such as coal combustion and vehicle exhaust. Compared with
those on the mountaintop relative abundances of NO_3^-, Mg^{2+} and Ca^{2+} in the DS II time
at the urban site were much more abundant, which can be attributed to heterogeneous
reactions of gaseous HNO_3, N_2O_5 and NO_x with the crustal alkaline metals in the dust
(Arimoto et al., 2004; Geng et al., 2009; Tobo et al., 2010; Triendl, 1998; Zamora et al.,
2011). Xi'an and Mt. Hua are located in the same latitude with a distance about 80 km,
and transport velocity of dust storm is generally very fast. Furthermore, DS II event
simultaneously occurred in Xi'an and Mt. Hua with a similar pattern of particle size
distribution (see the details in Fig. 9s and t and more discussion later). Therefore, it is
plausible that the differences in relative abundances of components of PM_{10} between
the urban and mountain sites can be ascribed to the reaction and/or adsorption of pol-
lutants from the local urban sources with dust during the DS II episode. Here we took
the mountain particle composition as a reference and calculated the aerosol production

from the urban pollutants during the event using the following equation.

$$A = C_i^{\text{Xi'an}} - \left[\frac{C_i^{\text{Mt. Hua}}}{PM_{10}^{\text{Mt. Hua}}} \right] \times PM_{10}^{\text{Xi'an}} \qquad (1)$$

Where A is the concentration of pollutant i formed from the local sources ($\mu g\,m^{-3}$), $C_i^{\text{Xi'an}}$ and $C_i^{\text{Mt. Hua}}$ are the concentrations of pollutant i in Xi'an and Mt. Hua during the event.

We found that in the DS II event 6.1, 2.1, 2.6, 7.7, 4.5 and 7.6 $\mu g\,m^{-3}$ of NO_3^-, SO_4^{2-}, NH_4^+, Ca^{2+}, EC and OC originated from the local urban sources, accounting for 57 %, 12 %, 66 %, 59 %, 87 % and 22 % of those in PM_{10} (see Table 2). Compared with that (2.1 $\mu g\,m^{-3}$, Table 2) of sulfate the local formed nitrate (6.1 $\mu g\,m^{-3}$, Table 2) during the DS II was about three times higher, again confirming a faster heterogeneous reaction of NO_x with dust, which largely occurs in particles with diameter larger than 3.3 μm (see more discussion below) and is consistent with the results reported previously (Phadnis and Carmichael, 2000).

To further recognize the sources of pollutants in Xi'an, major species in PM_{10} was analyzed using the statistic method of principal component analysis (PCA). As shown in Table 3, component 1 is of high loadings with F^-, Cl^-, K^+, WSOC, EC and OC, respectively, and represents fossil fuel and biomass combustion source, because F^-, K^+ and EC are largely derived from fossil fuel and biomass burning emission in China (Dan et al., 2004; Kline et al., 2004; Zhang et al., 2011). Component 2 represents dust emissions, because crustal species such as Na^+, Mg^{2+}, Ca^{2+}, and WSIC showed strong correlations with this factor. The coefficient of WSON with component 2 is 0.60, again indicating soil/dust is the major source especially in the dust storm periods. Component 3 displays high loadings with NO_3^-, SO_4^{2-} and NH_4^+, and thus represents a source of secondary formation. These three components explain 44 %, 29 % and 8 % of the total variance, respectively, and indicate fossil fuel/biomass combustion, soil/dust suspension and secondary formation as the major sources of PM_{10} in the city.

Title Page

Abstract | Introduction

Conclusions | References

Tables | Figures

◀ | ▶

◀ | ▶

Back | Close

Full Screen / Esc

Printer-friendly Version

Interactive Discussion

3.2 Size distribution

Almost all physicochemical and optical properties of aerosol are dependent on its size (Hinds, 1999). The size of ambient aerosol is not constant, which is always variable during the transport via various atmospheric processes such as coagulation, evapo-
ration, and adsorption/absorption (Herner et al., 2006). Detailed size distributions of particle mass (PM), inorganic ions and water-soluble organic (WSOC) and inorganic (WSIC) carbon during the nonevent and the event (DS II) are illustrated in Figs. 7 and 8, respectively. Their relative abundances in each size range are summarized in Table 4. Details in size distributions of major species during the same period in the troposphere
over Mt. Hua have been reported elsewhere (Wang et al., 2011c) and are cited here for a comparison.

3.2.1 During the non-dust storm period

Particle mass (PM) showed a bimodal pattern in Xi'an during the nonevent with coarse particles ($> 2.1\,\mu m$) as the major fraction (Fig. 7a), accounting for about 60 % of the
total particle mass (Table 4). Similar distribution was also found at the summit of Mt. Hua (Fig. 7b), suggesting an importance of coarse particles in the atmosphere over whole Guanzhong Basin in spring. Ammonium presented a unimodal pattern in the urban air with the highest peak at the size of 0.7–$1.1\,\mu m$ (Fig. 7c). Potassium ion showed a bimodal pattern with a major peak in the fine mode ($< 2.1\,\mu m$) and small peak in the
coarse mode ($> 2.1\,\mu m$) (Fig. 7e). Particulate ammonium is formed by a homogeneous reaction of ammonia with acidic gasses such HNO_3 and HCl and a subsequent partition into solid phase and/or a heterogeneous reaction of ammonia with aqueous sulfuric acid. Moreover, ammonia cannot react with coarse particles because of their alkaline nature. Therefore, a fine mode of ammonium was found at both sites (Fig. 7c, d). The
small fraction of ammonium in the coarse fraction is mostly derived from suspended soil containing fertilizer. Generally, fine mode of K^+ is mostly derived from biomass burning while the coarse mode K^+ can be attributed to suspended soil (Fig. 7e). Such

a soil-derived K^+ is less significant at the mountaintop, thus only a unimodal pattern was observed in the elevated troposphere (Fig. 7f). Mg^{2+} and Ca^{2+} are crust species, thus both showed a coarse mode between the boundary layer and the elevated troposphere (Fig. 7q–j). Na^+ is an important component in soil, thus it occurred abundantly in coarse fraction during the nonevent at both sites (Fig. 7k, l). The fine fraction of Na^+ can be explained by a biomass burning contribution, because biomass smoke contains a significant amount of Na_2SO_4 (Andreae et al., 1998). Cl^- showed an accumulation mode and a coarse mode in the urban area (Fig. 7m) but only exhibited a coarse mode in the mountain atmosphere (Fig. 7n). KCl is one of major species of airborne particulate Cl^-, which is produced in the biomass combustion process and emitted into the air as fine particles. During the ageing process of biomass burning plume KCl can react with gaseous HNO_3 and H_2SO_4 and release HCl into the air (Ikegami et al., 2001; Li et al., 2003; Pósfai et al., 2003). The gaseous HCl further transforms into aerosol phase by reaction with coarse particles (Hand et al., 2005; Tobo et al., 2010). Therefore, a bimodal pattern of Cl^- was obtained in the urban region (Fig. 7m). The disappeared peak of Cl^- in the fine mode at the mountain site indicates that the biomass burning derived aerosols was more aged when they arrived in the mountaintop (Fig. 7n). Because both are secondarily produced in the atmosphere, nitrate and sulfate are largely distributed in fine particles (Fig. 7o–r). The coarse mode of nitrate and sulfate can be attributable to uptake of gaseous HNO_3 and H_2SO_4 onto coarse particles. In addition, the coarse mode of sulfate is in part directly originated from soil since loess and desert dust also contain certain amount of sulfate (Sun et al., 2010). Ammonium nitrate is the major form of particulate NO_3^-, which is volatile and labile to decompose into gaseous NH_3 and HNO_3. As discussed above the reaction of SO_2 with OH radical to produce H_2SO_4 is slower compared to that of NO_x with OH to form HNO_3, thus it is expected that sulfate may be continuously formed during the transport of the precursors from the boundary layer to the free troposphere. The newly formed sulfate can displace the preexisting nitrate into the air, because sulfuric acid is the strongest and nonvolatile (Sullivian et al., 2007). Due to the above reasons nitrate is continuously redistributed from fine particles

onto coarse particle during long-range transport while sulfate remains in fine particles, resulting in the size distribution of nitrate changing into a bimodal pattern with two equivalent peaks in the fine and coarse fractions in the mountain air but no significant change for sulfate (Fig. 7p, r).

3.2.2 Dust storm on 24 April 2009 (DS II)

When dust was present all species in the urban air shifted toward larger sizes (Fig. 7s–ai), similar to those on the mountaintop (Fig. 7t–aj). Compared to those in the nonevent particle mass at both sites dominated in the coarse mode with a disappeared peak in the fine mode (Fig. 7s, t). Like that in the nonevent ammonium is still enriched in the fine mode, but a minor peak occurred in the coarse fraction (Fig. 7u, v), which can be attributed to fertilizer and biota in the dust. Ammonium in the size of 1.1–2.1 µm in Xi'an (Fig. 7u) and Mt. Hua (Fig. 7v) during the dust episode became less abundant compared to that in the nonevent at both sites (Fig. 7c, d), which is in part resulted from a less significant fine particle coagulation due to reduced residence time in the event compared with that in the nonevent (Wang et al., 2012a, b). Because K^+, Mg^{2+}, Ca^{2+} and Na^+ are originated from Gobi desert dust, these four ions dominated in the coarse mode in Xi'an during the event (Fig. 7w–ac), which is similar to those in the mountain atmosphere except K^+ (Fig. 7x–ad) and indicates a predominance of dust in the whole Guanzhong Basin from the boundary layer to the free troposphere during the DS II period. The fine mode of K^+ at Mt. Hua in the event is probably resulted from local biomass burning in the mountain area (Fig. 7x). As seen in Fig. 7ae, Cl^- presented a bimodal pattern with an increased coarse fraction in the event in Xi'an compared to that (Fig. 7m) in the nonevent. The fine mode Cl^- in the urban area during the event is mostly due to biomass burning emissions, whereas the coarse modes of Cl^- in the urban and the alpine atmospheres during the event are probably derived from the dried salt lakes in North China and Gobi regions. Size distribution pattern of nitrate in the urban air changed from a dominance in the fine mode during the nonevent into a bimodal pattern with two equivalent peaks in the fine and coarse ranges during

the DS II period (Fig. 7o, ag), indicating a significant shift of NO_3^- from fine particles into large dust during the episode. Such a redistribution was further pronounced in the mountain troposphere, resulting in a dominance in the coarse mode at Mt. Hua with no peak in the fine mode (Fig. 7ah). However, size distributions of sulfate at both sites were similar during the event with an increased peak in the coarse mode compared to those in the nonevent (Fig. 7ai, aj). The coarse mode of sulfate can be explained by an increasing input of dust, because dust particles from deserts in Northwest China and Gobi region contain a certain amount of sulfate (Sun et al., 2010). In addition, heterogeneous reaction of SO_2 with dust and/or uptake of H_2SO_4 onto dust may also be responsible for such a coarse mode of increase (Huang et al., 2012; Li et al., 2011; Sun et al., 2010; Takahashi et al., 2010; Zhang et al., 2003).

3.2.3 WSOC, WSIC and WSON in Xi'an

WSOC in the urban atmospheric particles presented a predominance in the fine mode with a small peak in the coarse mode during the nonevent, in contrast to a unimodal pattern of WSIC, which is dominant in the coarse mode (Fig. 8a–d). Several studies have reported that particulate WSOC in an urban environment is largely formed from photochemical oxidation of organic gases (Agarwal et al., 2010; Ram and Sarin, 2010; Salma et al., 2007; Wang et al., 2012a, b; Yu et al., 2004, 2005), thus a major peak was found in Xi'an during the non-dust storm period (Fig. 8a). The small peak of coarse mode of WSOC can be explained by a nature source such as pollen and soil (Fig. 8a), because water-soluble organic compounds like glucose (Graham et al., 2002; Wang et al., 2006a, b, 2009, 2011a, b) and humic acid (Brooks et al., 2004; Dinar et al., 2006; Havers et al., 1998) are enriched in these sources. During the dust storm period WSOC still displayed a bimodal pattern, but the fine mode significantly decreased while the coarse mode sharply increased as a dominant peak. Our previous study (Wang et al., 2012b) found that during the DS II period secondary organic aerosols in the Mt. Hua air were mostly formed from the local sources rather than being transported from the upwind region, and are of a size within the fine mode. However,

during the event primary organic aerosols such as water-soluble organic compounds like glucose and trehalose and water-insoluble organic compounds like high molecular weight (HMW) *n*-alkanes, fatty acids and fatty alcohols were derived from biota such as pollen, spore, invertebrate animals and plants in Gobi desert. Those Gobi dust de-
5   rived organic aerosols are of larger sizes and dominated in the downwind atmosphere in the event, resulting in a sharp increase in OC in the atmospheres of Mt. Hua and Mt. Tai in comparison to those in the nonevent (Wang et al., 2011c, 2012a, b). Therefore, a large peak in the coarse fraction and a small peak in the fine fraction were observed for WSOC in Xi'an in the DS II event (Fig. 8b).
10   As the major species of WSIC in the atmosphere, both carbonate (CO_3^{2-}) and bi-carbonate (HCO_3^-) ions are derived from soil and thus show a coarse mode in the nonevent (Fig. 8c). In the DS II time WSIC showed a bimodal pattern with a small peak in the fine mode and a large peak in the coarse mode (Fig. 8d). Such an increase of WSIC in the fine mode can be ascribed to an aqueous phase reaction of HNO_3/H_2SO_4
15   with fine calcite particles (Dunlea et al., 2009; Leaitch et al., 2009; Mcnaughton et al., 2009; Sullivan et al., 2007, 2009), which was 3.4 $\mu g\,m^{-3}$ in the DS II event and 10 times higher than that (0.3 ± 0.1 $\mu g\,m^{-3}$) in the nonevent.

Water-soluble organic nitrogen (WSON) are a class of complex nitrogen-containing compounds such as urea, amines, amino acids, eptides and proteins, which are de-
20   rived from urban pollution, biomass burning and dust (Altieri et al., 2012; Cape et al., 2011; Chen and Chen, 2010; Mace et al., 2003a, b; Violaki and Mihalopoulos, 2011; Zhang and Anastasio, 2003). WSON concentrated in fine particles as a unimodal pat-tern during the nonevent with 90 % of the total mass enriched in fine mode ($< 2.1\,\mu m$) (Fig. 8e and Table 4), which is similar to NH_4^+ (Fig. 7c). When dust was present WSON
25   exhibited a bimodal pattern with one peak in the fine mode and two peaks in the coarse mode (Fig. 8f). The coarse mode fraction accounts for 43 % of the total WSON, much more than that in the nonevent time (Table 4). Zamora et al. observed that compared to that in Barbados WSON in Miami increased by a factor of two when Sahara dust was present, although the actual dust concentrations at both cities were almost same

(Zamora et al., 2011). Similar results were also observed in Mediterranean (Mace et al., 2003a, b). The sharply enhanced WSON in Xi'an and the above documented phenomena suggest that WSON can be deposited onto dust particles via adsorption and/or coagulation. In addition, the coarse mode of WSON may also be directly originated from biological organisms in Gobi dust, which contains a certain amount of WSON species (Mace et al., 2003a, b).

3.3 Difference in aerosol acidity between Xi'an and Mt. Hua

Figure 9 plots the equivalent ratios of total measured ions in particle with different sizes in Xi'an. For particles with diameter less than 2.1 µm (Fig. 9a), the ratios of total cations to total anions were less than unity in both nonevent and event periods, suggesting an acidic nature of fine particles, but the slope of the regression line was smaller in the dust storm period (0.37) than in the non-dust period (0.80), indicating that fine particles in the event were more acidic. In Mt. Hua the slope of the regression line was 0.6 in the nonevent and increased to 0.9 on 24 April (Fig. 9b and the inserted figure), which means fine particles in the free troposphere became less acidic when dust was present. To our best knowledge, such an opposite trend of aerosol acidity between the boundary layer and free troposphere is found for the first time. We believed it is mostly caused by the difference in NO_3^- production. As mentioned above, NO_3^- is largely formed by oxidation of NO_2 with OH radical, which is much faster than the oxidation of SO_2 with OH to form SO_4^{2-} (Jockel et al., 2003; Rodhe et al., 1981; Seinfeld and Pandis, 1998). Atmospheric SO_4^{2-} can also be produced via heterogeneous reaction of SO_2 with H_2O_2 in cloud/aqueous phase, but the reaction rate ($k = 6 \times 10^{-16}$ cm^3 molec^{-1} s^{-1}) is still much lower than the NO_3^- production rate ($k = 8 \times 10^{-12}$ cm^3 molec^{-1} s^{-1}) (Rodhe et al., 1981). During the dust storm period the fast formed NO_3^- may quickly further react with calcite in dust to produce $Ca(NO_3)_2$. $Ca(NO_3)_2$ is hydrophilic and fine particulate $Ca(NO_3)_2$ can deliquescence above ~ 10 % RH (Tobo et al., 2010), which can further promote hydrolysis of other nitrogen oxides like N_2O_5 in the aqueous phase of aerosols

(He et al., 2012; Pathak et al., 2009), resulting in a significant formation of NO_3^- even in the dryer condition of the dust storm period. In addition, gaseous ammonia is sharply decreased due to the dilution effect of the prevailing winds in the event time. Therefore, the enhanced heterogeneous formation of NO_3^- and the decreased NH_4^+ led to the urban fine particles more acidic in the event than in the nonevent. However, the prevailing winds in the dust storm time prevented the boundary layer NO_x from being transported onto the mountain free troposphere, thus NO_3^- formation was depressed, resulting in the alpine fine particles becoming less acidic when dust was present. Such an increased acidity of airborne particles was also observed in other Chinese mega-cities such as Shanghai (Huang et al., 2010), Beijing and Chongqing (He et al., 2012) in the presence of dust storm.

Compared to those in the urban air the alpine aerosols are more aged due to long-range transport, thus in the nonevent fine particles in Mt. Hua are more acidic, rendering the cations/anions ratios smaller in Mt. Hua than in Xi'an (0.6 vs. 0.8) (Fig. 9a, b). During the nonevent coarse particles showed similar acidic characteristic at both sites; particles in the size of 2.1–5.8 µm are slightly acidic or neutral, but particles with a size larger than 5.8 µm are basic (Fig. 9c). On the contrary, all the coarse particles in the mountain air were almost neutral during the nonevent and became basic when dust occurred (Fig. 9d). Because NO_3^-, SO_4^{2-}, NH_4^+ and Ca^{2+} are major ions of aerosols at both sites, here we compare their relative abundance to further discuss the acidity difference of aerosols between the urban ground surface and the mountain troposphere (Fig. 10). Equivalent ratio of NO_3^-/SO_4^{2-} in fine particles from Xi'an was 0.51 ± 0.13 (Fig. 10a) and 0.63 (Fig. 10c) in the nonevent and the event periods, respectively, again demonstrating an enhanced production of NO_3^- during the dust storm period. Although NH_4^+ relative to the sum of $[NO_3^- + SO_4^{2-}]$ decreased in the event at Mt. Hua, the total abundance of NH_4^+ plus Ca^{2+} relative to $[NO_3^- + SO_4^{2-}]$ increased in the event (Fig. 10c), being opposite to those in Xi'an. During ageing process NH_4NO_3 can be evaporated into the air and decomposed as NH_3 and HNO_3 while NH_4HSO_4 and $(NH_4)_2SO_4$ are chemically stable and enriched in fine particles. The gaseous HNO_3 further react with coarse

Title Page

Abstract	Introduction
Conclusions	References
Tables	Figures

◀◀   ▶▶

◀   ▶

Back   Close

Full Screen / Esc

Printer-friendly Version

Interactive Discussion

particle and enhances the coarse fractions of NO_3^- and Ca^{2+} in the non-dust period (Fig. 10b and Table 4). Such a significant segregation of nitrate from sulfate was also observed in the outflow region of East Asia (Sullivian et al., 2007). Nitrate is formed at a faster rate than sulfate and long-range transport of nitrate is less pronounced than that of sulfate. Therefore, NO_3^-/SO_4^{2-} in the coarse mode was lower when dust storm occurred especially in the mountainous area (Fig. 10d). NH_4^+, NO_3^- and SO_4^{2-} are the three major ions in fine particle. As shown in Fig. 11, the equivalent ratio of $[NO_3^- + HSO_4^{2-}]$ to NH_4^+ is close to unity, thus it seems plausible that ammonium in the nonevent existed mainly as NH_4NO_3 and NH_4HSO_4 rather than $(NH4)_2SO_4$. As discussed above fine particles in the event are more acidic, suggesting ammonium in the event was more deficient. The above results suggest that the difference in acidity of particles between the nonevent and the event occurred only in the fine mode.

4   Summary and conclusion

Springtime of PM_{10} and size-segregated samples collected in Xi'an were determined for EC, OC, WSOC, WSON and inorganic ions, and compared with those simultaneously measured on the mountaintop of Mt. Tai. Particle mass (PM), EC, OC and inorganic ions in Xi'an were 1.8–22 times higher than those in the Mt. Hua air during the non-dust storm period and 1.2–9.2 times higher than those in the mountainous air during the DS II period. High level of WSON was found in the DS II time due to the deposition of anthropogenic WSON onto dust and the input of biological organism in Gobi desert dust. Compared with those in Xi'an during the nonevent aerosols in the mountaintop free troposphere contains more sulfate and less nitrate, which is due to continuous formation of sulfate and decomposition of nitrate during aerosol ageing. In the nonevent time sulfate was the most abundant species in aerosols from Xi'an and Mt. Hua, followed by nitrate, OC and ammonium. On the contrary, OC became

Impact of Gobi desert dust on aerosol chemistry of Xi'an

G. H. Wang et al.

the highest in the event at both sites, followed by SO_4^{2-}, Ca^{2+} and NO_3^-, indicating the importance of input of biota in Gobi desert.

In the nonevent time PM showed a similar size distribution between the urban boundary layer and the mountain free troposphere with two equivalent peaks in the fine and coarse modes. In contrast, PM became a unimodal pattern in both regions in the DS II period, dominating in coarse mode. NH_4^+, K^+, Mg^{2+}, Ca^{2+}, Na^{2+} in Xi'an exhibited similar size distribution patterns to those in the mountain air. Cl^- and NO_3^- showed a bimodal pattern on the ground surface and shifted onto large particles in the mountain troposphere during the nonevent period. Such a redistribution was significantly enhanced when dust occurred, resulting in Cl^- and NO_3^- almost entirely staying in the coarse mode in the mountain air.

Compared to those in the nonevent acidity of fine aerosols in the event became more acidic in the urban air and less acidic in the mountain elevated atmosphere. The increased acidity in Xi'an is largely ascribed to an enhanced heterogeneous formation of NO_3^- and a decreased level of NH_3 caused by a dilution effect of the prevailing northerly winds in the DS II time. However, such a NO_3^- formation was depressed in the mountain air in the event, because the prevailing northerly winds prohibited NO_x being transported from ground surface to the mountain atmosphere. In the mountain air coarse particles were almost entirely neutralized in the nonevent and became more basic in the presence of dust storm. In contrast, coarse particles with diameter between 2.1–5.8 µm were still acidic during the whole sampling period in Xi'an and those with diameter > 5.8 µm were basic.

Impact of Gobi desert dust on aerosol chemistry of Xi'an

G. H. Wang et al.

Title Page

Abstract	Introduction
Conclusions	References
Tables	Figures

◀◀   ▶▶

◀   ▶

Back   Close

Full Screen / Esc

Printer-friendly Version

Interactive Discussion

References

Agarwal, S., Aggarwal, S. G., Okuzawa, K., and Kawamura, K.: Size distributions of dicarboxylic acids, ketoacids, α-dicarbonyls, sugars, WSOC, OC, EC and inorganic ions in atmospheric particles over Northern Japan: implication for long-range transport of Siberian biomass burning and East Asian polluted aerosols, Atmos. Chem. Phys., 10, 5839–5858, doi:10.5194/acp-10-5839-2010, 2010.

Altieri, K. E., Hastings, M. G., Peters, A. J., and Sigman, D. M.: Molecular characterization of water soluble organic nitrogen in marine rainwater by ultra-high resolution electrospray ionization mass spectrometry, Atmos. Chem. Phys., 12, 3557–3571, doi:10.5194/acp-12-3557-2012, 2012.

Andreae, M. O., Andreae, T. W., Annegarn, H., Beer, J., Cachier, H., Lecanut, P., Elbert, W., Maenhaut, W., Salma, I., Wienhold, F. G., and Zenker, T.: Airborne studies of aerosol emissions from savanna fires in Southern Africa: 2. aerosol chemical composition, J. Geophys. Res., 103, 32119–32128, 1998.

Arimoto, R., Zhang, X. Y., Huebert, B. J., Kang, C. H., Savoie, D. L., Prospero, J. M., Sage, S. K., Schloesslin, C. A., Khaing, H. M., and Oh, S. N.: Chemical composition of atmospheric aerosols from Zhenbeitai, China, and Gosan, South Korea, during ACE-Asia, J. Geophys. Res.-Atmos., 109, D19S04, doi:10.1029/2003JD004323, 2004.

Arimoto, R., Kim, Y. J., Kim, Y. P., Quinn, P. K., Bates, T. S., Anderson, T. L., Gong, S., Uno, I., Chin, M., Huebert, B. J., Clarke, A. D., Shinozuka, Y., Weber, R. J., Anderson, J. R., Guazzotti, S. A., Sullivan, R. C., Sodeman, D. A., Prather, K. A., and Sokolik, I. N.: Characterization of Asian dust during ACE-Asia, Global Planet. Change, 52, 23–56, 2006.

Brooks, S. D., Demott, P. J., and Kreidenweis, S. M.: Water uptake by particles containing humic materials and mixtures of humic materials with ammonium sulfate, Atmos. Environ., 38, 1859–1868, 2004.

Cape, J. N., Cornell, S. E., Jickells, T. D., and Nemitz, E.: Organic nitrogen in the atmosphere – where does it come from? A review of sources and methods, Atmos. Res., 102, 30–48, 2011.

Chen, H. Y. and Chen, L. D.: Occurrence of water soluble organic nitrogen in aerosols at a coastal area, J. Atmos. Chem., 65, 49–71, 2010.

Title Page

Abstract | Introduction

Conclusions | References

Tables | Figures

◀ | ▶

◀ | ▶

Back | Close

Full Screen / Esc

Printer-friendly Version

Interactive Discussion

Chow, J. C., Watson, J. G., Chen, L.-W. A., Arnott, W. P., Moosmuller, H., and Fung, K. K.: Equivalence of elemental carbon by thermal/optical reflectance and transmittance with different temperature protocols, Environ. Sci. Technol., 38, 4414–4422, 2004.

Chow, J. C., Watson, J. G., Chen, L.-W. A., Chang, M. C. O., Robinson, N. F., Trimble, D., and Kohl, S.: The IMPROVE temperature protocol for thermal/optical carbon analysis: maintaining consistency with a long-term database, J. Air Waste Manage., 57, 1014–1023, 2007.

Dan, M., Zhuang, G., Li, X., Tao, H., and Zhuang, Y.: The characteristics of carbonaceous species and their sources in $PM_{2.5}$ in Beijng, Atmos. Environ., 38, 3443–3452, 2004.

Dillner, A. M., Schauer, J. J., Zhang, Y., Zeng, L., and Cass, G. R.: Size-resolved particulate matter composition in Beijing during pollution and dust events, J. Geophys. Res., 111, D05203, doi:10.1029/2005JD006400, 2006.

Dinar, E., Mentel, T. F., and Rudich, Y.: The density of humic acids and humic like substances (HULIS) from fresh and aged wood burning and pollution aerosol particles, Atmos. Chem. Phys., 6, 5213–5224, doi:10.5194/acp-6-5213-2006, 2006.

Dunlea, E. J., DeCarlo, P. F., Aiken, A. C., Kimmel, J. R., Peltier, R. E., Weber, R. J., Tomlinson, J., Collins, D. R., Shinozuka, Y., McNaughton, C. S., Howell, S. G., Clarke, A. D., Emmons, L. K., Apel, E. C., Pfister, G. G., van Donkelaar, A., Martin, R. V., Millet, D. B., Heald, C. L., and Jimenez, J. L.: Evolution of Asian aerosols during transpacific transport in INTEX-B, Atmos. Chem. Phys., 9, 7257–7287, doi:10.5194/acp-9-7257-2009, 2009.

Formenti, P., Schütz, L., Balkanski, Y., Desboeufs, K., Ebert, M., Kandler, K., Petzold, A., Scheuvens, D., Weinbruch, S., and Zhang, D.: Recent progress in understanding physical and chemical properties of African and Asian mineral dust, Atmos. Chem. Phys., 11, 8231–8256, doi:10.5194/acp-11-8231-2011, 2011.

Geng, H., Park, Y., Hwang, H., Kang, S., and Ro, C.-U.: Elevated nitrogen-containing particles observed in Asian dust aerosol samples collected at the marine boundary layer of the Bohai Sea and the Yellow Sea, Atmos. Chem. Phys., 9, 6933–6947, doi:10.5194/acp-9-6933-2009, 2009.

Graham, B., Mayol-Bracero, O. L., Guyon, P., Roberts, G. C., Decesari, S., Facchini, M. C., Artaxo, P., Maenhaut, W., Koll, P., and Andreae, M. O.: Water-soluble organic compounds in biomass burning aerosols over Amazonia – 1. Characterization by NMR and GC-MS, J. Geophys. Res.-Atmos., 107, 8047, doi:10.1029/2001JD000336, 2002.

Hand, J. L., Malm, W. C., Laskin, A., Day, D., Lee, T., Wang, C., Carrico, C., Carrillo, J., Cowin, J. P., Collett-Jr, J., and Iedema, M. J.: Optical, physical, and chemical properties

of tar balls observed during the Yosemite Aerosol Characterization Study, J. Geophys. Res.-Atmos., 110, D21210, doi:10.21029/22004JD005728, 2005.

Havers, N., Burba, P., Lambert, J., and Klockow, D.: Characterization of humic-like substances in airborne particulate matter, J. Atmos. Chem., 29, 45–54, 1998.

He, K., Zhao, Q., Ma, Y., Duan, F., Yang, F., Shi, Z., and Chen, G.: Spatial and seasonal variability of PM$_{2.5}$ acidity at two Chinese megacities: insights into the formation of secondary inorganic aerosols, Atmos. Chem. Phys., 12, 1377–1395, doi:10.5194/acp-12-1377-2012, 2012.

Herner, J. D., Ying, Q., Aw, J., Gao, O., Chang, D. P. Y., and Kleeman, M. J.: Dominant mechanism that shape the airborne particle size and composition distribution in Central California, Aerosol Sci. Tech., 40, 827–844, 2006.

Hinds, W. C.: Aerosol Technology: Properties, Behavior, and Measurement of Airborne Particles, John Willy & Sons, New York, 1999.

Huang, K., Zhuang, G., Li, J., Wang, Q., Sun, Y., Lin, Y., and Fu, J. S.: Mixing of Asian dust with pollution aerosol and the transformation of aerosol components during the dust storm over China in spring 2007, J. Geophys. Res.-Atmos., 115, D00K13, doi:10.1029/2009JD013145, 2010.

Huang, K., Zhuang, G., Lin, Y., Fu, J. S., Wang, Q., Liu, T., Zhang, R., Jiang, Y., Deng, C., Fu, Q., Hsu, N. C., and Cao, B.: Typical types and formation mechanisms of haze in an Eastern Asia megacity, Shanghai, Atmos. Chem. Phys., 12, 105–124, doi:10.5194/acp-12-105-2012, 2012.

Huebert, B. J., Bates, T., Russell, P. B., Shi, G. Y., Kim, Y. J., Kawamura, K., Carmichael, G., and Nakajima, T.: An overview of ACE-Asia: strategies for quantifying the relationships between Asian aerosols and their climatic impacts, J. Geophys. Res.-Atmos., 108, D238663, doi:10.1029/2003JD003550, 2003.

Ikegami, M., Okada, K., Zaizen, Y., Makino, Y., Jensen, J. B., Gras, J. L., and Harjanto, H.: Very high weight ratios of S/K in individual haze particles over Kalimantan during the 1997 Indonesian forest fires, Atmos. Environ., 35, 4237–4243, 2001.

Jacobson, M. Z.: Global direct radiative forcing due to multicomponent anthropogenic and natural aerosols, J. Geophys. Res.-Atmos., 106, 1551–1568, 2001.

Jöckel, P., Brenninkmeijer, C. A. M., and Crutzen, P. J.: A discussion on the determination of atmospheric OH and its trends, Atmos. Chem. Phys., 3, 107–118, doi:10.5194/acp-3-107-2003, 2003.

Title Page

Abstract | Introduction

Conclusions | References

Tables | Figures

◄ | ►

Back | Close

Full Screen / Esc

Printer-friendly Version

Interactive Discussion

Karagulian, F., Santschi, C., and Rossi, M. J.: The heterogeneous chemical kinetics of N_2O_5 on $CaCO_3$ and other atmospheric mineral dust surrogates, Atmos. Chem. Phys., 6, 1373–1388, doi:10.5194/acp-6-1373-2006, 2006.

Kline, J., Huebert, B., Howell, S., Blomquist, B., Zhuang, J., Bertram, T., and Carrillo, J.: Aerosol composition and size versus altitude measured from the C-130 during ACE-Asia, J. Geophys. Res.-Atmos., 109, D19S08, doi:10.1029/2004JD004540, 2004.

Leaitch, W. R., Macdonald, A. M., Anlauf, K. G., Liu, P. S. K., Toom-Sauntry, D., Li, S.-M., Liggio, J., Hayden, K., Wasey, M. A., Russell, L. M., Takahama, S., Liu, S., van Donkelaar, A., Duck, T., Martin, R. V., Zhang, Q., Sun, Y., McKendry, I., Shantz, N. C., and Cubison, M.: Evidence for Asian dust effects from aerosol plume measurements during INTEX-B 2006 near Whistler, BC, Atmos. Chem. Phys., 9, 3523–3546, doi:10.5194/acp-9-3523-2009, 2009.

Li, J., Pósfai, M. L., Hobbs, P. V., and Buseck, P. R.: Individual aerosol particles from biomass burning in Southern Africa: 2. Compositions and aging of inorganic particles, J. Geophys. Res., 108, 8484, doi:10.1029/2002JD002310, 2003.

Li, J. J., Wang, G. H., Zhou, B. H., Cheng, C. L., Cao, J. J., Shen, Z. X., and An, Z. S.: Chemical composition and size distribution of wintertime aerosols in the atmosphere of Mt. Hua in Central China, Atmos. Environ., 45, 1251–1258, 2011.

Mace, K. A., Artaxo, P., and Duce, R. A.: Water-soluble organic nitrogen in Amazon Basin aerosols during the dry (biomass burning) and wet seasons, J. Geophys. Res., 108, 4512, doi:10.1029/2003JD003557, 2003a.

Mace, K. A., Kubilay, N., and Duce, R. A.: Organic nitrogen in rain and aerosol in the Eastern Mediterranean atmosphere: an association with atmospheric dust, J. Geophys. Res.-Atmos., 108, 4320, doi:10.1029/2002JD002997, 2003b.

Manktelow, P. T., Carslaw, K. S., Mann, G. W., and Spracklen, D. V.: The impact of dust on sulfate aerosol, CN and CCN during an East Asian dust storm, Atmos. Chem. Phys., 10, 365–382, doi:10.5194/acp-10-365-2010, 2010.

McNaughton, C. S., Clarke, A. D., Kapustin, V., Shinozuka, Y., Howell, S. G., Anderson, B. E., Winstead, E., Dibb, J., Scheuer, E., Cohen, R. C., Wooldridge, P., Perring, A., Huey, L. G., Kim, S., Jimenez, J. L., Dunlea, E. J., DeCarlo, P. F., Wennberg, P. O., Crounse, J. D., Weinheimer, A. J., and Flocke, F.: Observations of heterogeneous reactions between Asian pollution and mineral dust over the Eastern North Pacific during INTEX-B, Atmos. Chem. Phys., 9, 8283–8308, doi:10.5194/acp-9-8283-2009, 2009.

Impact of Gobi desert dust on aerosol chemistry of Xi'an

G. H. Wang et al.

Title Page

Abstract	Introduction
Conclusions	References
Tables	Figures

|◄ | ►|

◄ | ►

Back | Close

Full Screen / Esc

Printer-friendly Version

Interactive Discussion

Mogili, P. K., Kleiber, P. D., Young, M. A., and Grassian, V. H.: N_2O_5 hydrolysis on the components of mineral dust and sea salt aerosol: comparison study in an environmental aerosol reaction chamber, Atmos. Environ., 40, 7401–7408, 2006.

Pathak, R. K., Wu, W. S., and Wang, T.: Summertime $PM_{2.5}$ ionic species in four major cities of China: nitrate formation in an ammonia-deficient atmosphere, Atmos. Chem. Phys., 9, 1711–1722, doi:10.5194/acp-9-1711-2009, 2009.

Peltier, R. E., Hecobian, A. H., Weber, R. J., Stohl, A., Atlas, E. L., Riemer, D. D., Blake, D. R., Apel, E., Campos, T., and Karl, T.: Investigating the sources and atmospheric processing of fine particles from Asia and the Northwestern United States measured during INTEX B, Atmos. Chem. Phys., 8, 1835–1853, doi:10.5194/acp-8-1835-2008, 2008.

Phadnis, M. J., and Carmichael, G. R.: Numerical investigation of the influence of mineral dust on the tropospheric chemistry of East Asia, J. Atmos. Chem., 36, 285–323, 2000.

Pósfai, M., Simonics, R., Li, J., Hobbs, P. V., and Buseck, P. R.: Individual aerosol particles from biomass burning in Southern Africa: 1. compositions and size distributions of carbonaceous particles, J. Geophys. Res.-Atmos., 103, 8483, doi:10.1029/2002JD002291, 2003.

Ram, K. and Sarin, M. M.: Spatio-temporal variability in atmospheric abundances of EC, OC and WSOC over Northern India, J. Aerosol Sci., 41, 88–98, 2010.

Rodhe, H., Crutzen, P., and Vanderpol, A.: Formation of sulfuric and nitric acid in the atmosphere during long-range transport, Tellus, 33, 132–141, 1981.

Salma, I., Ocskay, R., Chi, X., and Maenhaut, W.: Sampling artefacts, concentration and chemical composition of fine water-soluble organic carbon and humic-like substances in a continental urban atmospheric environment, Atmos. Environ., 41, 4106–4118, 2007.

Seinfeld, J. H. and Pandis, S. N.: Atmoshperic Chemistry and Physics, John Wiley & Sons, New York, 1998.

Seinfeld, J. H., Carmichael, G. R., Arimoto, R., Conant, W. C., Brechtel, F. J., Bates, T. A., Cahill, T. A., Clarke, A. D., Doherty, S. J., Flatau, P. J., Huebert, B. J., Kim, J., Markowicz, K. M., Quinn, P. K., Russell, L. M., Russell, P. B., Shimizu, A., Shinozuka, Y., Song, C. H., Tang, Y. H., Uno, I., Vogelmann, A. M., Weber, R. J., Woo, J. H., and Zhang, X. Y.: ACE-Asia: regional climatic and atmospheric chemical effects of Asian dust and pollution, B. Am. Meteorol. Soc., 85, 367–380, doi:doi:10.1175/BAMS-85-3-367, 2004.

Simoneit, B. R. T., Kobayashi, M., Mochida, M., Kawamura, K., and Huebert, B. J.: Aerosol particles collected on aircraft flights over the Northwestern Pacific region during the ACE-

Title Page

Abstract | Introduction

Conclusions | References

Tables | Figures

|◄ | ►|

◄ | ►

Back | Close

Full Screen / Esc

Printer-friendly Version

Interactive Discussion

Discussion Paper | Discussion Paper | Discussion Paper | Discussion Paper

Asia campaign: composition and major sources of the organic compounds, J. Geophys. Res.-Atmos., 109, D19S09, doi:10.1029/2004JD004565, 2004a.

Simoneit, B. R. T., Kobayashi, M., Mochida, M., Kawamura, K., Lee, M., Lim, H. J., Turpin, B. J., and Komazaki, Y.: Composition and major sources of organic compounds of aerosol particulate matter sampled during the ACE-Asia campaign, J. Geophys. Res.-Atmos., 109, D19S10, doi:10.1029/2004JD004598, 2004b.

Sullivan, R. C., Guazzotti, S. A., Sodeman, D. A., and Prather, K. A.: Direct observations of the atmospheric processing of Asian mineral dust, Atmos. Chem. Phys., 7, 1213–1236, doi:10.5194/acp-7-1213-2007, 2007.

Sullivan, R. C., Moore, M. J. K., Petters, M. D., Kreidenweis, S. M., Roberts, G. C., and Prather, K. A.: Effect of chemical mixing state on the hygroscopicity and cloud nucleation properties of calcium mineral dust particles, Atmos. Chem. Phys., 9, 3303–3316, doi:10.5194/acp-9-3303-2009, 2009.

Sun, Y., Zhuang, G., Huang, K., Li, J., Wang, Q., Wang, Y., Lin, Y., Fu, J. S., Zhang, W., Tang, A., and Zhao, X.: Asian dust over Northern China and its impact on the downstream aerosol chemistry in 2004, J. Geophys. Res., 115, D00K09, doi:10.1029/2009jd012757, 2010.

Takahashi, H., Naoe, H., Igarashi, Y., Inomata, Y., and Sugimoto, N.: Aerosol concentrations observed at Mt. Haruna, Japan, in relation to long-range transport of Asian mineral dust aerosols, Atmos. Environ., 44, 4638–4644, 2010.

Tobo, Y., Zhang, D., Matsuki, A., and Iwasaka, Y.: Asian dust particles converted into aqueous droplets under remote marine atmospheric conditions, P. Natl. Acad. Sci. USA, 107, 17905–17910, 2010.

Triendl, R.: Asian states take "first step" on acid rain, Nature, 392, 426–426, 1998.

Van Donkelaar, A., Martin, R. V., Brauer, M., Kahn, R., Levy, R., Verduzco, C., and Villeneuve, P. J.: Global estimates of ambient fine particulate matter concentrations from satellite-based aerosol optical depth: development and application, Environ. Health Persp., 118, 8347–8355, 2010.

van Donkelaar, A., Martin, R. V., Leaitch, W. R., Macdonald, A. M., Walker, T. W., Streets, D. G., Zhang, Q., Dunlea, E. J., Jimenez, J. L., Dibb, J. E., Huey, L. G., Weber, R., and Andreae, M. O.: Analysis of aircraft and satellite measurements from the Intercontinental Chemical Transport Experiment (INTEX-B) to quantify long-range transport of East Asian sulfur to Canada, Atmos. Chem. Phys., 8, 2999–3014, doi:10.5194/acp-8-2999-2008, 2008.

Impact of Gobi desert dust on aerosol chemistry of Xi'an

G. H. Wang et al.

Title Page

Abstract | Introduction

Conclusions | References

Tables | Figures

◄ | ►

◄ | ►

Back | Close

Full Screen / Esc

Printer-friendly Version

Interactive Discussion

Vancuren, R. A. and Cahill, T. A.: Asian aerosols in North America: frequency and concentration of fine dust, J. Geophys. Res., 107, 4804, doi:10.1029/2002JD002204, 2002.

Violaki, K. and Mihalopoulos, N.: Water-soluble organic nitrogen (WSON) in size-segregated atmospheric particles over the Eastern Mediterranean, Atmos. Environ., 44, 4339–4345, 2010.

Violaki, K. and Mihalopoulos, N.: Urea: an important piece of Water Soluble Organic Nitrogen (WSON) over the Eastern Mediterranean, Sci. Total Environ., 409, 4796–4801, 2011.

Vrekoussis, M., Kanakidou, M., Mihalopoulos, N., Crutzen, P. J., Lelieveld, J., Perner, D., Berresheim, H., and Baboukas, E.: Role of the NO_3 radicals in oxidation processes in the Eastern Mediterranean troposphere during the MINOS campaign, Atmos. Chem. Phys., 4, 169–182, doi:10.5194/acp-4-169-2004, 2004.

Vrekoussis, M., Mihalopoulos, N., Gerasopoulos, E., Kanakidou, M., Crutzen, P. J., and Lelieveld, J.: Two-years of NO_3 radical observations in the boundary layer over the Eastern Mediterranean, Atmos. Chem. Phys., 7, 315–327, doi:10.5194/acp-7-315-2007, 2007.

Wang, G., Kawamura, K., Umemoto, N., Xie, M., Hu, S., and Wang, Z.: Water-soluble organic compounds in $PM_{2.5}$ and size-segregated aerosols over Mt. Tai in North China Plain, J. Geophys. Res.-Atmos., 114, D19208, doi:10.1029/2008JD011390, 2009.

Wang, G., Xie, M., Hu, S., Gao, S., Tachibana, E., and Kawamura, K.: Dicarboxylic acids, metals and isotopic compositions of C and N in atmospheric aerosols from inland China: implications for dust and coal burning emission and secondary aerosol formation, Atmos. Chem. Phys., 10, 6087–6096, doi:10.5194/acp-10-6087-2010, 2010.

Wang, G., Chen, C., Li, J., Zhou, B., Xie, M., Hu, S., Kawamura, K., and Chen, Y.: Molecular composition and size distribution of sugars, sugar-alcohols and carboxylic acids in airborne particles during a severe urban haze event caused by wheat straw burning, Atmos. Environ., 45, 2473–2479, 2011a.

Wang, G., Kawamura, K., Hu, S., Xie, M., Zhou, B., Li, J., Cao, J., and An, Z.: Selected water-soluble organic compounds found in size-resolved aerosols collected from the urban, mountain, and marine atmospheres over East Asia, Tellus B, 63, 371–381, 2011b.

Wang, G., Li, J., Cheng, C., Hu, S., Xie, M., Gao, S., Zhou, B., Dai, W., Cao, J., and An, Z.: Observation of atmospheric aerosols at Mt. Hua and Mt. Tai in central and east China during spring 2009 – Part 1: EC, OC and inorganic ions, Atmos. Chem. Phys., 11, 4221–4235, doi:10.5194/acp-11-4221-2011, 2011c.

Wang, G., Kawamura, K., Cao, J., Zhang, R., Cheng, C., Li, J., Zhang, T., Liu, S., and Zhao, Z.: Molecular distribution and stable carbon isotopic composition of dicarboxylic acids, ketocar-

Impact of Gobi desert dust on aerosol chemistry of Xi'an

G. H. Wang et al.

Title Page

Abstract	Introduction
Conclusions	References
Tables	Figures

|◄ | ►|

◄ | ►

Back | Close

Full Screen / Esc

Printer-friendly Version

Interactive Discussion

boxylic acids and α-dicarbonyls in size-resolved atmospheric particles from Xi'an city, China, Environ. Sci. Technol., 46, 4783–4791, 2012a.

Wang, G. H., Kawamura, K., Lee, S. C., Ho, K. F., and Cao, J. J.: Molecular, seasonal and spatial distributions of organic aerosols from fourteen Chinese cities, Environ. Sci. Technol., 40, 4619–4625, 2006a.

Wang, G. H., Kawamura, K., Watanabe, T., Lee, S. C., Ho, K. F., and Cao, J. J.: Heavy loadings and source strengths of organic aerosols in China, Geophys. Res. Lett., 33, L22801, doi:10.1029/2006GL027624, 2006b.

Wang, G. H., Li, J. J., Cheng, C. L., Zhou, B. H., Xie, M. J., Hu, S. Y., Meng, J. J., Sun, T., Ren, Y. Q., Cao, J. J., Liu, S. X., Zhang, T., and Zhao, Z. Z.: Observation of atmospheric aerosols at Mt. Hua and Mt. Tai in Central and East China during spring 2009 – Part 2: Impact of dust storm on organic aerosol composition and size distribution, Atmos. Chem. Phys., 12, 4065–4080, doi:10.5194/acp-12-4065-2012, 2012b.

Yu, J. Z., Yang, H., Zhang, H., and Lau, A. K. H.: Size distributions of water-soluble organic carbon in ambient aerosols and its size-resolved thermal characteristics, Atmos. Environ., 38, 1061–1071, 2004.

Yu, J. Z., Huang, X. F., Xu, J. H., and Hu, M.: When aerosol sulfate goes up, so does oxalate: implication for the formation mechanisms of oxalate, Environ. Sci. Technol., 39, 128–133, 2005.

Zamora, L. M., Prospero, J. M., and Hansell, D. A.: Organic nitrogen in aerosols and precipitation at Barbados and Miami: implications regarding sources, transport and deposition to the Western Subtropical North Atlantic, J. Geophys. Res., 116, D20309, doi:10.1029/2011JD015660, 2011.

Zhang, Q. and Anastasio, C.: Free and combined amino compounds in atmospheric fine particles ($PM_{2.5}$) and fog waters from Northern California, Atmos. Environ., 37, 2247–2258, 2003.

Zhang, D. Z., Zang, J. Y., Shi, G. Y., Iwasaka, Y., Matsuki, A., and Trochkine, D.: Mixture state of individual Asian dust particles at a coastal site of Qingdao, China, Atmos. Environ., 37, 3895–3901, 2003.

Zhang, T., Cao, J. J., Tie, X. X., Shen, Z. X., Liu, S. X., Ding, H., Han, Y. M., Wang, G. H., Ho, K. F., Qiang, J., and Li, W. T.: Water-soluble ions in atmospheric aerosols measured in Xi'an, China: Seasonal variations and sources, Atmos. Res., 102, 110–119, 2011.

Title Page

Abstract | Introduction

Conclusions | References

Tables | Figures

◄ | ►

Back | Close

Full Screen / Esc

Printer-friendly Version

Interactive Discussion

ACPD

12, 21355–21397, 2012

Impact of Gobi
desert dust on
aerosol chemistry of
Xi'an

G. H. Wang et al.

Title Page

Abstract | Introduction

Conclusions | References

Tables | Figures

◄ | ►►

◄ | ►

Back | Close

Full Screen / Esc

Printer-friendly Version

Interactive Discussion

Table 1. Concentrations of water-soluble species, elemental carbon (EC) and organic carbon (OC) of PM_{10} during the spring 2009 in Xi'an, China.

| | Non-dust storm period | | | | | | | | Dust storm event period | | | | |
| | Daytime (N = 29) | | | | Nighttime (N = 31) | | | | DS I (N = 1) | DS II (N = 3) | | | |
	Min	Max	Mean	Std	Min	Max	Mean	Std		Min	Max	Mean	Std
PM_{10}	58	420	250	79	110	415	263	90	527	358	890	589	273
pH^a	−1.1	0.2	−0.3	0.3	−1.0	0.1	−0.4	0.3	0.4	−0.1	0.1	0.0	0.1
F^-	0.0	1.3	0.5	0.3	0.1	1.1	0.5	0.3	0.3	0.1	0.6	0.4	0.2
Cl^-	0.4	11	2.9	2.5	0.6	15	6.1	3.9	4.1	1.1	4.7	3.0	1.8
NO_3^-	4.0	72	27	17	4.0	66	24	18	6.0	5.7	19	11	7.0
SO_4^{2-}	8.0	88	33	17	8.9	82	30	18	17	7.5	27	17	10
Na^+	0.1	3.1	1.1	0.6	0.2	3.9	1.3	0.8	5.0	0.4	3.4	2.1	1.5
NH_4^+	2.0	24	11	5.0	2.1	23	10	5.2	1.8	1.6	8.6	3.9	4.0
K^+	0.6	5.3	2.1	1.0	1.1	4.8	2.4	1.0	1.4	0.8	1.8	1.3	0.5
Mg^{2+}	0.1	1.1	0.5	0.2	0.1	1.2	0.6	0.3	1.1	0.9	1.9	1.3	0.6
Ca^{2+}	0.8	14	8.5	3.5	0.9	16	8.0	3.8	16	11	16	13	2.7
$WSOC^b$	4.7	25	16	4.4	8.1	29	17	5.3	6.4	13	23	16	5.6
$WSIC^b$	1.2	11	4.6	2.7	1.3	14	4.7	3.2	13	3.8	24	13	10
$WSTN^c$	11	42	20	7.3	11	39	20	7.1	11	16	31	24	7.0
$WSON^c$	3.8	8.1	5.6	1.1	3.7	22	6.5	3.4	8.1	5.5	28	19	12
EC	2.6	23	10	4.8	4.9	29	14	7.5	5.5	2.3	8.1	5.2	2.9
OC	7.9	38	23	7.4	12	67	28	12	29	21	43	35	12
OC/EC	1.6	4.7	2.5	0.6	1.5	4.5	2.3	0.7	5.3	5.0	9.1	7.5	2.2
WSOC/OC	0.4	0.9	0.7	0.2	0.3	0.9	0.6	0.2	0.2	0.3	0.6	0.5	0.1
WSON/WSTN	0.1	0.7	0.3	0.2	0.1	0.8	0.4	0.2	0.7	0.3	0.9	0.8	0.3
WSOC/WSON	0.6	6.2	3.0	1.2	1.0	6.4	3.0	1.3	0.8	0.5	2.5	0.8	1.0

[a] pH = pH value of water-extracts of sample – pH value of the field blank;
[b] WSOC and WSIC are water-soluble organic and inorganic carbon;
[c] WSTN is water-soluble total nitrogen and WSON is WSTN – N of NH_4^+ and NO_3^-.

Table 2. Concentrations of species derived from local sources and their relative abundance to the total in PM$_{10}$ samples of Xi'an during the dust storm event (DS II, 24 April 2009).

	F$^-$	Cl$^-$	NO$_3^-$	SO$_4^{2-}$	NH$_4^+$	K$^+$	Mg^{2+}	Ca^{2+}	EC	OC
Concentrations of species from local sources, µg m^{-3}	0.3	2.0	6.1	2.1	2.6	0.77	0.76	7.7	4.5	7.6
Relative abundance to the total in PM$_{10}$, %	87	67	57	12	66	59	61	59	87	22

Table 3. Principal component analysis for PM_{10} of Xi'an during the whole sampling period ($N = 64$).

	Component		
	1	2	3
PM_{10}	0.27	**0.92**	0.10
F^-	**0.80**[a]	0.28	0.14
Cl^-	**0.88**	0.12	0.16
NO_3^-	0.25	−0.04	**0.92**
SO_4^{2-}	0.19	0.08	**0.93**
Na^+	0.23	**0.65**	0.04
NH_4^+	0.22	−0.17	**0.95**
K^+	**0.72**	0.11	**0.61**
Mg^{2+}	0.34	**0.89**	0.11
Ca^{2+}	0.34	**0.78**	−0.12
WSOC	**0.62**	0.22	0.40
WSIC	−0.09	**0.68**	**−0.62**
EC	**0.90**	0.07	0.33
OC	**0.83**	0.47	0.04
WSON	−0.21	**0.60**	−0.38
%Variance	44 %	29 %	8 %

[a] Absolute values more than 0.5 are highlighted in bold.

Table 4. Concentration percentage (%) of particle mass (PM), inorganic ions, water-soluble organic carbon (WSOC), water-soluble inorganic carbon (WSIC) and water-soluble organic nitrogen (WSON) in the size-resolved aerosols from Xi'an and Mt. Hua during the spring of 2009.

Size range, μm	PM	F^-	Cl^-	NO_3^-	SO_4^{2-}	Na^+	NH_4^+	K^+	Mg^{2+}	Ca^{2+}	WSOC	WSIC	WSON
					I. Non-dust storm period								
					(a) Xi'an ($N = 5$)								
> 9.0	23 ± 4.9	24 ± 2.8	10 ± .4	6.9 ± 2.5	7.5 ± 1.4	11 ± 1.9	0.5 ± 0.1	2.8 ± 1.5	25 ± 4.3	35 ± 5.5	4.4 ± 3.3	37 ± 4.1	0.7 ± 1.2
5.8–9.0	14 ± 1.2	22 ± 4.7	11 ± 2.9	6.8 ± 1.3	6.2 ± 1.5	14 ± 6.1	0.3 ± 0.2	6.1 ± 6.8	22 ± 5.3	27 ± 4.5	4.5 ± 4.8	25 ± 7.5	1.3 ± 1.1
4.7–5.8	7.5 ± 2.3	15 ± 1.6	7.7 ± 2.9	4.0 ± 0.8	3.3 ± 0.4	6.4 ± 2.5	0.2 ± 0.1	0.0 ± 0.0	11 ± 1.4	9.9 ± 2.0	5.4 ± 4.5	16 ± 4.4	1.0 ± 0.6
3.3–4.7	9.9 ± 2.8	21 ± 1.8	9.4 ± 4.2	6.3 ± 2.1	4.2 ± 0.4	9.5 ± 2.9	0.8 ± 0.3	1.0 ± 0.8	12 ± 0.9	9.7 ± 1.0	3.3 ± 1.3	12 ± 0.7	2.6 ± 0.4
2.1–3.3	7.3 ± 3.2	14 ± 1.9	8.1 ± 1.5	6.5 ± 1.0	5.2 ± 0.4	11 ± 1.8	2.2 ± 0.3	3.5 ± 1.8	9.0 ± 0.8	6.3 ± 0.7	4.3 ± 1.6	2.9 ± 0.6	3.2 ± 0.6
1.1–2.1	13 ± 1.2	1.8 ± 2.9	16 ± 3.4	24 ± 3.2	24 ± 3.1	19 ± 3.4	29 ± 4.3	26 ± 6.1	10 ± 0.5	4.7 ± 0.5	17 ± 3.6	1.8 ± 0.7	20 ± 4.4
0.7–1.1	13 ± 2.9	0.0 ± 0.0	15 ± 3.3	25 ± 3.5	26 ± 1.9	10 ± 5.7	36 ± 1.9	27 ± 7.9	5.5 ± 0.7	4.1 ± 1.1	26 ± 11	1.3 ± 0.8	40 ± 8.9
0.4–0.7	8.1 ± 1.6	0.0 ± 0.0	15 ± 7.1	16 ± 1.7	16 ± 1.4	10 ± 1.2	23 ± 1.8	24 ± 10	3.4 ± 0.3	2.2 ± 1.0	28 ± 15	2.0 ± 0.6	23 ± 1.5
< 0.4	4.5 ± 0.4	2.1 ± 3.3	8.2 ± 3.8	5.3 ± 1.0	7.8 ± 1.6	8.1 ± 1.2	8.1 ± 2.2	9.9 ± 7.1	2.4 ± 0.4	1.2 ± 0.9	7.1 ± 2.5	3.2 ± 1.5	8.1 ± 3.0
Total	100	100	100	100	100	100	100	100	100	100	100	100	100
					(b) Mt. Hua ($N = 3$)								
> 9.0	19 ± 2.4	40 ± 25	52 ± 14	15 ± 3.4	7.3 ± 6.0	20 ± 3.4	3.1 ± 3.2	4.7 ± 3.6	23 ± 11	27 ± 12	NA[a]	NA	NA
5.8–9.0	13 ± 1.1	25 ± 6.5	25 ± 16	12 ± 4.1	4.5 ± 1.9	11 ± 6.1	1.9 ± 1.4	2.5 ± 0.7	15 ± 2.0	18 ± 2.8	NA	NA	NA
4.7–5.8	7.3 ± 0.6	5.6 ± 4.9	8.2 ± 13	5.8 ± 1.9	3.1 ± 1.1	10 ± 6.0	1.0 ± 0.5	1.5 ± 1.8	7.6 ± 0.5	8.8 ± 1.6	NA	NA	NA
3.3–4.7	10 ± 1.0	19 ± 6.5	5.4 ± 9.3	13 ± 3.9	4.3 ± 1.3	14 ± 2.2	2.1 ± 1.1	2.6 ± 0.8	14 ± 1.3	15 ± 2.5	NA	NA	NA
2.1–3.3	8.1 ± 0.5	6.3 ± 6.1	7.6 ± 13	10 ± 2.1	4.7 ± 1.0	11 ± 3.6	2.8 ± 1.7	3.6 ± 1.4	13 ± 2.6	11 ± 3.2	NA	NA	NA
1.1–2.1	13 ± 1.6	3.2 ± 5.5	1.3 ± 2.3	15 ± 3.3	18 ± 4.5	15 ± 2.0	20 ± 4.9	23 ± 6.2	16 ± 3.9	8.4 ± 1.7	NA	NA	NA
0.7–1.1	15 ± 1.4	0.1 ± 0.1	0.0 ± 0.0	16 ± 5.3	30 ± 7.1	8.3 ± 2.3	35 ± 4.7	35 ± 3.2	6.6 ± 1.6	4.5 ± 0.4	NA	NA	NA
0.4–0.7	9.4 ± 1.5	0.3 ± 0.5	0.0 ± 0.0	8.9 ± 2.8	18 ± 4.8	9.2 ± 4.2	22 ± 6.0	20 ± 6.6	3.0 ± 1.2	3.6 ± 0.7	NA	NA	NA
< 0.4	5.5 ± 1.9	0.0 ± 0.0	0.0 ± 0.0	3.8 ± 2.4	9.1 ± 4.2	0.8 ± 1.4	11 ± 5.4	7.7 ± 5.4	1.7 ± 0.3	2.6 ± 0.7	NA	NA	NA
Total	100	100	100	100	100	100	100	100	100	100	NA	NA	NA
					II. Dust storm period (DS II, 24 April 2009)								
					(a) Xi'an ($N = 1$)								
> 9.0	23	ND[b]	23	7.0	13	18	1.4	93	21	31	31	16	0.3
5.8–9.0	21	ND	12	6.2	14	27	0.9	4.2	19	27	16	20	17
4.7–5.8	11	ND	8.1	11	8.2	20	1.7	0.2	12	11	11	11	0.3
3.3–4.7	16	ND	8.1	9.3	9.9	14	4.4	1.9	13	14	13	16	13
2.1–3.3	12	ND	7.7	12	9.1	6.3	3.2	0.0	11	11	13	9.6	12
1.1–2.1	8.2	ND	11	17	14	9.8	17	0.0	8.9	3.8	1.4	7.5	6.7
0.7–1.1	4.3	ND	12	21	14	0.0	29	1.1	7.1	2.6	11	5.4	0.3
0.4–0.7	2.7	ND	9.4	9.0	10	2.5	25	0.0	4.0	0.0	2.3	7.8	33
< 0.4	2.1	ND	8.5	7.7	9.1	3.4	18	0.0	3.6	0.0	1.6	6.6	17
Total	100	ND	100	100	100	100	100	100	100	100	100	100	100
					(b) Mt. Hua ($N = 1$)								
> 9.0	30	ND	33	13	20	28	6.9	16	23	21	NA	NA	NA
5.8–9.0	20	ND	24	13	14	25	4.9	11	18	16	NA	NA	NA
4.7–5.8	11	ND	9.6	8.4	7.5	11	2.5	4.6	10	12	NA	NA	NA
3.3–4.7	16	ND	21	23	12	21	5.3	13	19	20	NA	NA	NA
2.1–3.3	11	ND	10	20	8.7	11	5.0	9.4	13	15	NA	NA	NA
1.1–2.1	6.8	ND	1.5	12	10	2.6	8.8	14	10	11	NA	NA	NA
0.7–1.1	2.1	ND	0.0	4.1	12	0.4	32	17	2.7	2.4	NA	NA	NA
0.4–0.7	1.4	ND	0.0	2.9	8.7	0.2	22	10	1.7	2.0	NA	NA	NA
< 0.4	1.1	ND	0.0	3.2	5.7	0.0	13	5.4	0.8	1.1	NA	NA	NA
Total	100	ND	100	100	100	100	100	100	100	100	NA	NA	NA

[a] NA: not available due to limited materials on the sample filter;

[b] ND: not determined.

Title Page

Abstract | Introduction

Conclusions | References

Tables | Figures

◀ | ▶

◀ | ▶

Back | Close

Full Screen / Esc

Printer-friendly Version

Interactive Discussion
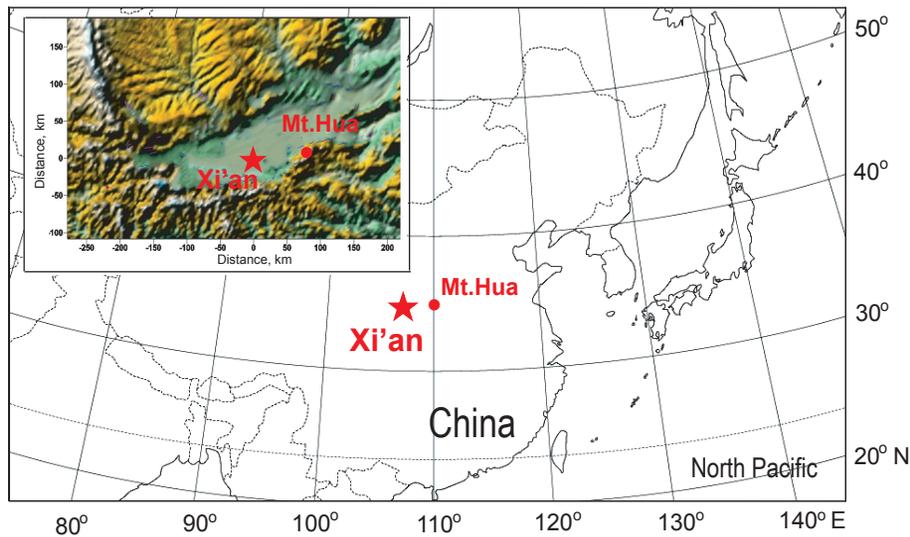
Fig. 1. A map description for Xi'an city and Mt. Hua in Guanzhong Basin, Central China (inserted figure showing the topography of Guanzhong Basin).
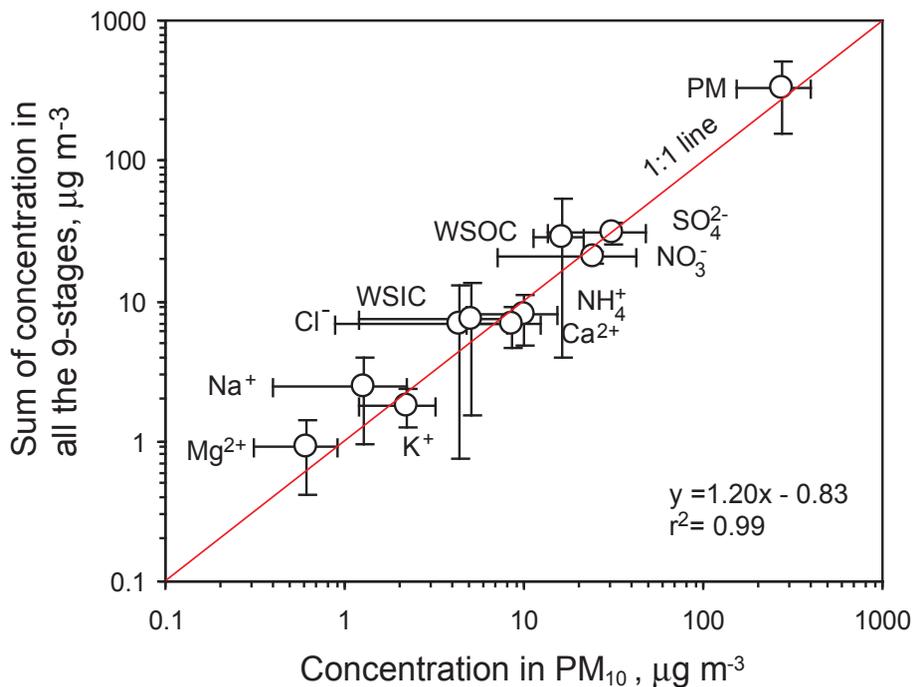
Fig. 2. Intercomparison of components measured by the PM_{10} sampler and the 9-stage sampler during the campaign.

Title Page

Abstract | Introduction

Conclusions | References

Tables | Figures

|◄ | ►|

◄ | ►

Back | Close

Full Screen / Esc

Printer-friendly Version

Interactive Discussion
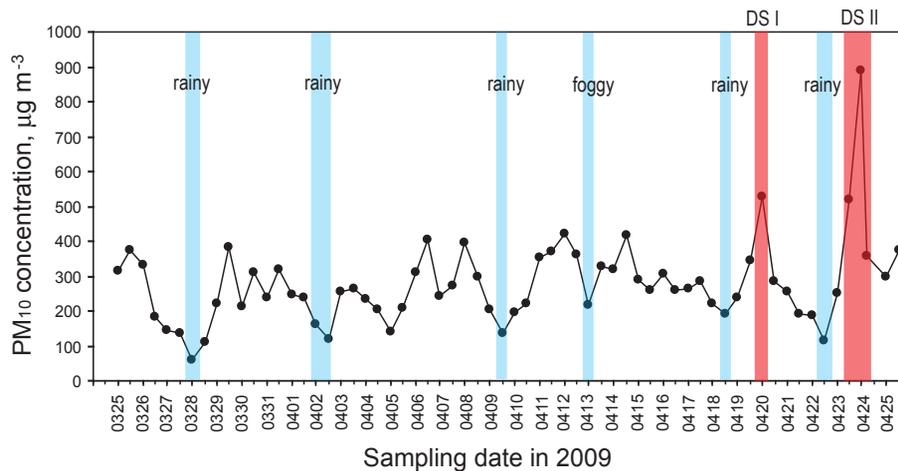
Fig. 3. Temporal variation of PM_{10} in Xi'an during the spring of 2009 (DS I and DS II in red color represent the two dust storm events occurring on 20 and 24 April, respectively).

(I) Non-dust period

(II) Dust storm period
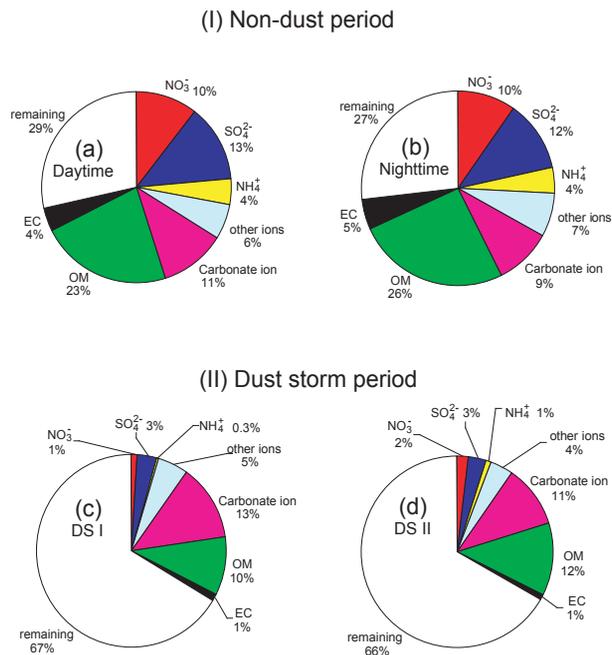
Fig. 4. Mass closure of PM$_{10}$ during the sampling periods (OM: organic matter = OC × 1.6).

Fig. 5. Differences in concentrations of components of PM_{10} from Xi'an and Mt. Hua during the non-dust and dust storm periods (inserted numbers are the concentration ratios of Xi'an to Mt. Hua).

Title Page

Abstract | Introduction

Conclusions | References

Tables | Figures

|◀ | ▶|

◀ | ▶

Back | Close

Full Screen / Esc

Printer-friendly Version

Interactive Discussion
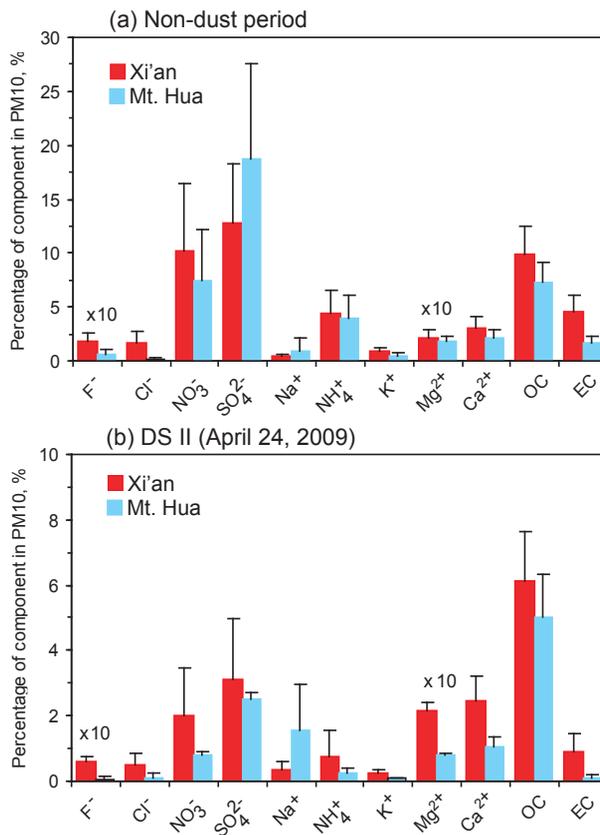
Full Screen / Esc

Fig. 6. Relative abundances of components of PM_{10} from Xi'an and Mt. Hua during **(a)** the non-dust storm and **(b)** the dust storm periods.
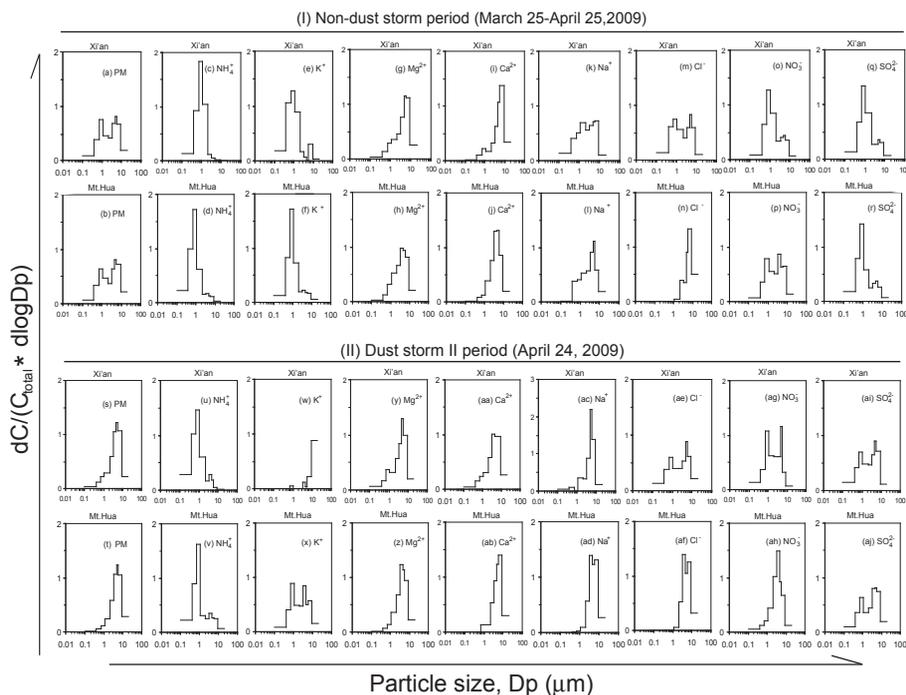
Fig. 7. Differencs in size distributions of particle mass (PM) and inorganic ions in the atmospheres of Xi'an and Mt. Hua during (I) the non-dust storm and (II) the dust storm periods.
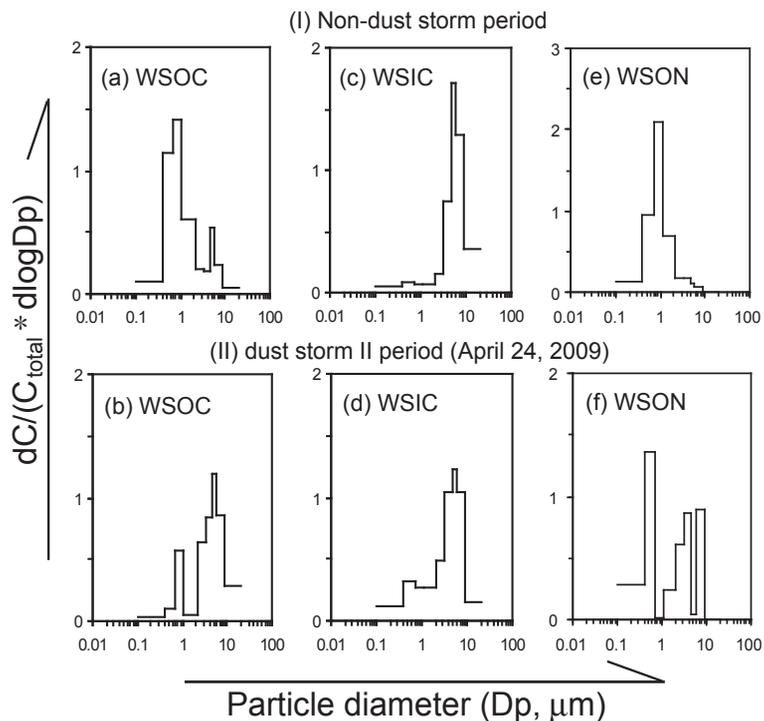
Fig. 8. Size distribution of water-soluble organic carbon (WSOC), inorganic carbon (WSIC) and organic nitrogen (WSON) in Xi'an during (I) the non-dust storm and (II) the dust storm periods.
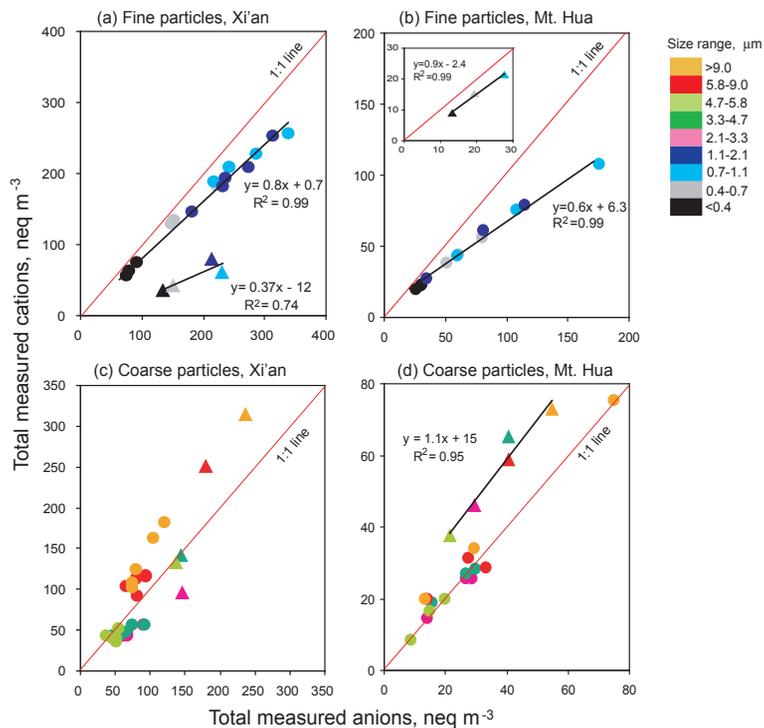
Fig. 9. Acidity of size-segregated samples in Xi'an and Mt. Hua during the non-dust storm (circle symbols) and dust storm (24 April 2009, triangle symbols) periods.
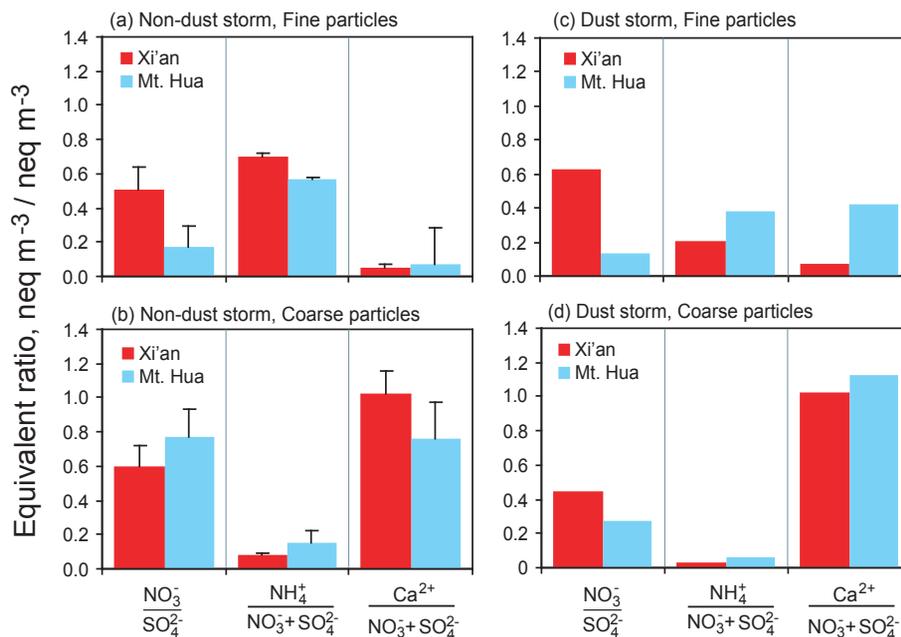
Fig. 10. Equivalent ratios of major inorganic ions in fine ($< 2.1\,\mu m$) and coarse ($> 2.1\,\mu m$) particles from Xi'an and Mt. Hua during **(a, b)** non-dust storm and **(c, d)** dust storm (24 April 2009, DS II) periods.
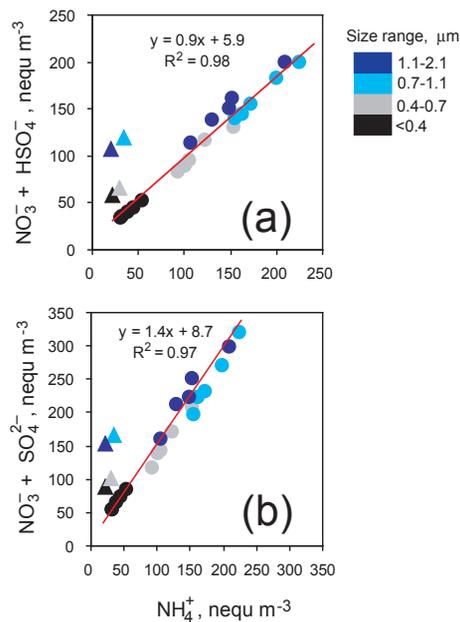
Fig. 11. Linear fit regression for ions in fine particles (< 2.1 μm) during the non-dust storm (circle symbols) and dust storm (24 April 2009, triangle symbols) periods in Xi'an.